

MICROCOPY RESOLUTION TEST CHART
NATIONAL BUREAU OF STANDARDS-1963-A

12

AD-A160 619

Spectrally Selective Shutter Mechanism

E. F. CROSS, G. D. WIEMOKLY, and O. L. GIBB
Aerophysics Laboratory

and

W. A. GARBER
Electronics Research Laboratory
Laboratory Operations
The Aerospace Corporation
El Segundo, CA 90245

9 September 1985

DTIC
ELECTE
OCT 29 1985
S B

APPROVED FOR PUBLIC RELEASE;
DISTRIBUTION UNLIMITED

DTIC FILE COPY

Prepared for
SPACE DIVISION
AIR FORCE SYSTEMS COMMAND
Los Angeles Air Force Station
P.O. Box 92960, Worldway Postal Center
Los Angeles, CA 90009-2960

This report was submitted by The Aerospace Corporation, El Segundo, CA 90245, under Contract No. F04701-83-C-0084 with the Space Division, P.O. Box 92960, Worldway Postal Center, Los Angeles, CA 90009-2960. It was reviewed and approved for The Aerospace Corporation by W. P. Thompson, Jr., Director, Aerophysics Laboratory. Captain Mark D. Borchardt, SD/YNV, was the project officer for the Mission-Oriented Investigation and Experimentation Program.

This report has been reviewed by the Public Affairs Office (PAS) and is releasable to the National Technical Information Service (NTIS). At NTIS, it will be available to the general public, including foreign nationals.

This technical report has been reviewed and is approved for publication. Publication of this report does not constitute Air Force approval of the report's findings or conclusions. It is published only for the exchange and stimulation of ideas.

Mark D. Borchardt
Mark D. Borchardt, Captain, USAF
Project Officer

Joseph Hess
Joseph Hess, GM-15, Director, West Coast
Office, AF Space Technology Center

UNCLASSIFIED

SECURITY CLASSIFICATION OF THIS PAGE (When Data Entered)

REPORT DOCUMENTATION PAGE		READ INSTRUCTIONS BEFORE COMPLETING FORM
1. REPORT NUMBER SD-TR-85-48	2. GOVT ACCESSION NO. A160 619	3. RECIPIENT'S CATALOG NUMBER
4. TITLE (and Subtitle) SPECTRALLY SELECTIVE SHUTTER MECHANISM	5. TYPE OF REPORT & PERIOD COVERED	
	6. PERFORMING ORG. REPORT NUMBER TR-0084A(5930-01)-2	
7. AUTHOR(s) Edward F. Cross, Gary D. Wiemokly, Owen L. Gibb, and Wilbur A. Garber	8. CONTRACT OR GRANT NUMBER(s) FO4701-83-C-0084	
9. PERFORMING ORGANIZATION NAME AND ADDRESS The Aerospace Corporation El Segundo, Calif. 90245	10. PROGRAM ELEMENT, PROJECT, TASK AREA & WORK UNIT NUMBERS	
11. CONTROLLING OFFICE NAME AND ADDRESS Space Division Los Angeles Air Force Station Los Angeles, Calif. 90009-2960	12. REPORT DATE 9 September 1985	
	13. NUMBER OF PAGES 41	
14. MONITORING AGENCY NAME & ADDRESS (if different from Controlling Office)	15. SECURITY CLASS. (of this report) Unclassified	
	15a. DECLASSIFICATION/DOWNGRADING SCHEDULE	
16. DISTRIBUTION STATEMENT (of this Report) Approved for public release; distribution unlimited.		
17. DISTRIBUTION STATEMENT (of the abstract entered in Block 20, if different from Report)		
18. SUPPLEMENTARY NOTES		
19. KEY WORDS (Continue on reverse side if necessary and identify by block number) Dual filter shuttering Filter shuttering in the visible and infrared spectrum Infrared shutter mechanism Rotating filter shutter Shuttering systems using spectral filters		
20. ABSTRACT (Continue on reverse side if necessary and identify by block number) Several state-of-the-art detection and image systems require synchronous high-speed shuttering of incoming irradiance. This shuttering action is necessary in many instances to increase signal-to-noise ratio, obtain high-speed (low-retention) imagery, and provide single-event observations. Presently, this type of "snap-shot" imagery is approximated by rotating chopper wheel methods that sweep an aperture across the focal plane. At faster aperture rates, these mechanical chopper systems become more complex and maintenance of image fidelity is very difficult. This novel,		

DD FORM 1473
(FACSIMILE)

UNCLASSIFIED

SECURITY CLASSIFICATION OF THIS PAGE (When Data Entered)

19. KEY WORDS (Continued)

Spectral filter shuttering
Spectral shutter mechanism
Spectral shuttering with visible and infrared filters
Spectrally selective chopper technique
Two filters for synchronous chopping

20. ABSTRACT (Continued)

spectrally selective shutter mechanism provides true "snap-shot" imagery. Despite some limitations, such a mechanism is ideally suited to high flux, high background, and rapidly changing imaging visualization, and can be used to monitor flow visualization, chemiluminescence phenomena, and laser operation.

The optomechanical technique described in this report uses the rotation of one or two narrowband spectral filters to provide open-shutter times in the millisecond range. The resulting performance of the two-filter assembly is governed by the physical principle that increasing angular tilt of a narrowband interference filter causes the bandpass parameter to shift progressively toward shorter wavelengths. *Keywords: infrared filters*

Data presented in this report demonstrate that the spectral shutter technique can provide repetitive open-shutter times in the low-millisecond range, with true "snap-shot" images synchronized to video rates. Both advantages and limitations of this spectrally selective shutter are discussed and compared to typical mechanical chopper wheel methods. Specifically, performance advantages include the capability to provide (1) "snap-shot" imagery that always encompasses the entire field of view, (2) self-contained spectral selectivity for focused signal irradiance, (3) greater transmission efficiency during open-shutter times, and (4) adaptability to a wider variety of optical systems.

FIGURES

1.	Filter Angular Geometry for Dual-Planar Filter.....	10
2.	Comparison between Single- and Dual-Planar Tilt with Identical Filters.....	11
3.	Filter I Transmission Scans for 0 to 35° Tilt Angles θ_T	14
4.	Filter I Bandpass Parameters (λ_0 , T_{eff} , and $\Delta\lambda$) as a Function of Angular Tilt θ_T	15
5.	Transmission Scans for 0 to 38° Tilt Angles θ_T	16
6.	Filter III Transmission Scans for 0 to 38° Tilt Angles θ_T	17
7.	Filter II Bandpass Parameters (λ_0 , T_{eff} , and $\Delta\lambda$) as a Function of Angular Tilt θ_T	18
8.	Filter III Bandpass Parameters (λ_0 , T_{eff} , and $\Delta\lambda$) as a Function of Angular Tilt θ_T	19
9.	Spectral Shutter Design A, a Stationary and Rotational Filter Combination Using Single-Planar Tilt at the Optical Aperture.....	21
10.	Spectral Shutter Design A with Filter I Composite Trans- mission Profiles for Filter Angular Displacements.....	22
11.	Spectral Shutter Design A with Filter I Composite Trans- mission Efficiency versus Tilt Angle θ_T	23
12.	Spectral Shutter Design B, a Stationary and Rotational Filter Combination Using Dual-Planar Tilt at the Optical Aperture.....	25
13.	Transmission Scans for Filters I and I' at Angular Coincidence.....	26
14.	Spectral Shutter Design B with Filters I and I' Composite Transmission Profiles for Filter Angular Displacement.....	27
15.	Spectral Shutter Design B with Filter I Composite Trans- mission Efficiency T_{eff} versus Tilt Angle θ_T	28
16.	Spectral Shutter Design C, a Stationary Filter near the Focal Plane and a Rotating Filter with Dual-Planar Tilt at the Optical Aperture.....	29
17.	Spectral Shutter Design D, a Double Rotational Filter Combination Using Single-Planar Tilt at the Optical Aperture.....	30

FIGURES (Continued)

18.	Spectral Shutter Design D with Filter I Composite Transmission Profiles for Filter Angular Displacements.....	32
19.	Spectral Shutter Design D with Filter I Composite Transmission Efficiency T_{eff} versus Tilt Angle θ_T	33
20.	Spectral Shutter Design D with Filters II and III Composite Transmission Profiles for Filter Angular Displacements.....	34
21.	Spectral Shutter Design D with Filters II and III Composite Transmission Efficiency T_{eff} versus Tilt Angle θ_T	35

I. INTRODUCTION

Several detection and image systems require synchronous high-speed shuttering of incoming irradiance levels. This operational mode is specifically employed to (1) provide blur-free imagery of rapidly moving targets, (2) restrict far-field background irradiance to integration times less than the framing rate, and (3) allow viewing of rapid changes in scene intensity fluctuations and distributions that occur within the image frame-time. Such "shuttered" imagery is currently obtained with a rotating chopper wheel installed over the focal plane. However, the increased chopper wheel size and speed required to produce submillisecond shuttering presents a more difficult design problem. Furthermore, this conventional electromechanical approach observes the field of view sequentially during the sweeping motion of the chopper wheel aperture. As a result, video output corresponding to irradiance levels can be significantly distorted by changes in image intensity and position that occur when the aperture is open.

The novel technique described in this report achieves repetitive open-shutter periods that are in the submillisecond range. This range of shutter speed is almost an order of magnitude faster than is realizable with a conventional chopper wheel. Unlike mechanical shutters, this technique produces true "snap-shot" imagery over the entire optical field of view. Since narrow-band filters are used in this optomechanical approach, the open-shutter time is spectrally selective.

This new shutter mechanism can be used in applications where it is necessary to obtain (1) blur-free imagery of rapidly changing scenes or (2) spectrally selective chopper action at television rates or higher without significant system changes. Camera systems can incorporate this shuttering feature to monitor explosive detonation, high-velocity collisions, and targets rapidly traversing the optical field of view. The spectral selectivity of the shuttering makes it ideally suited for observing flow visualization and chemiluminescence phenomena in laser research studies. Possible space applications of this technique involve the recognition and tracking of targets that fluctuate very rapidly in location and intensity. Also, an image system with this high-speed synchronous shuttering could be set up to monitor and track targets irradiated with a pulsed laser beam.

II. THEORY OF OPERATION

The fast optomechanical shutter described in this report uses the rotation of one or two bandpass filters. The resulting performance is based on the physical principle that increasing tilt angle between a narrowband interference filter and the optical focal plane causes the filter bandpass to shift toward shorter wavelengths. This optical effect results from apparent increases in thin-film coating thicknesses as filter tilt angle increases relative to incoming irradiance. Inventors E. F. Cross, M. A. Kwok, and D. C. Jonuska used this same optical phenomenon to develop a technique for multispectral imaging with an infrared television (see Ref. 1). Furthermore, Optical Coating Laboratory, Inc. (OCLI) has issued a technical report discussing the effects of incident angle on infrared filter characteristics (see Ref. 2).

An interference filter is made of thin-film multilayers that act essentially as individual Fabry-Perot interferometers. The manufacturer produces these layers (such as quarter-wave plates) to create optical interference for a given wavelength. For small-angle approximation, the bandpass remains constant; but for larger angles (greater than 10° for most filters), the optical phase thickness and reflection coefficients change. The electromagnetic theory found in Fresnel's equations governs the reflectance and transmittance in the filter, while the optical phase thickness, proportional to a cosine function, governs interference.

For narrowband interference filters, the amount of downward spectral shift in filter bandpass characteristics is determined by the absolute value of angular tilt θ_T . This decrease in filter cut-on, cut-off, and center wavelengths (λ_1 , λ_2 , and λ_0 , respectively) with increased tilt is accompanied by a decrease in peak transmission efficiency T_{eff} and a slight widening of bandwidth $\Delta\lambda$. Both the aforementioned are more discernible in a visible-light filter than in infrared filters. In general, all the above spectral effects become more definitive when the filter angular tilt becomes greater than 20° . A second-order effect is the polarization of irradiance transmitted through an

interference filter tilted at a large incident angle. This phenomenon makes it unsatisfactory to use the dual-filter configuration as a shutter in front of optics having a large field of view (i.e., greater than 40°).

Continuous decrease in bandpass wavelengths as a function of θ_T can be repetitively accomplished with a motor that rotates the narrowband filter about either axis, parallel to the focal plane. With two such filters set up in tandem over the camera optics, irradiance transmission can be limited to the rotational time during which spectral bandpass characteristics for both filters are approximately equal. Outside this time period, filter attenuation and mechanical baffling combine to completely block scene irradiance. The filter tilt angles at which maximum irradiance is transmitted through the two-filter assembly are defined as the coincident tilt angles $\theta_T(C1)$ and $\theta_T(C2)$. Filters used in this shuttering mechanism should have the desired open-aperture bandpass characteristics at a tilt angle where the change in peak wavelength transmission as a function of tilt angle, $\partial\lambda_0/\partial\theta_T$, begins increasing rapidly. Under these conditions the time differential required to go from fully open to fully closed aperture is very sharply defined without the usual sweeping action of a mechanical shutter that sequentially masks parts of the image plane.

For every θ_T , resultant transmission efficiency $T_{eff}(R)$ through the two-filter configuration is the product of the transmission efficiency for each filter at θ_T [$T_{eff}(\theta_{T1})$ and $T_{eff}(\theta_{T2})$]. The equation for this calculation is

$$T_{eff}(R) = T_{eff}(\theta_{T1}) \cdot T_{eff}(\theta_{T2})$$

For the specific open-aperture condition, peak shutter transmission $T_{eff}(S)$ is the product of the peak transmissions for both filters at angular coincidence $T_{eff}(C1)$ and $T_{eff}(C2)$, as expressed by the equation

$$T_{eff}(S) = T_{eff}(C1) \cdot T_{eff}(C2)$$

The open-shutter time t_{os} for each image is calculated from the following equation

$$t_{os} = \frac{\partial t}{\partial \theta_M} (\theta_U - \theta_L)$$

where $\frac{\partial t}{\partial \theta_M}$ is the time necessary for the revolving filter to traverse a 1° angle, θ_U^M is the increased tilt angle (in degrees) required to reach 10% of $T_{eff}(S)$, and θ_L is the decreased tilt angle (in degrees) required to reach 10% of $T_{eff}(S)$.

Since bandpass characteristics are governed by the filter's angular position relative to incident irradiance (incident angle), a two-dimensional (dual-planar) filter tilt can be designed that is spectrally dependent on initial filter tilt and angular rotation. A filter with dual-planar tilt (see Fig. 1) forms a three-angle Eulerian system, with the two angles (initial tilt and filter rotation) adding vectorally to give the resultant incident angle. This two-dimensional filter positioning creates a varying bandpass whose upper wavelength is limited by the initial tilt angle of the rotating filter. This novel filter orientation is very advantageous to an optomechanical shutter design, since the bandpass of the rotating filter does not change rapidly until after the first few (typically 10) degrees. As an example, Fig. 2 shows the equivalent spectral transmission scans that result from a single- and dual-planar tilt of a typical narrowband interference filter.

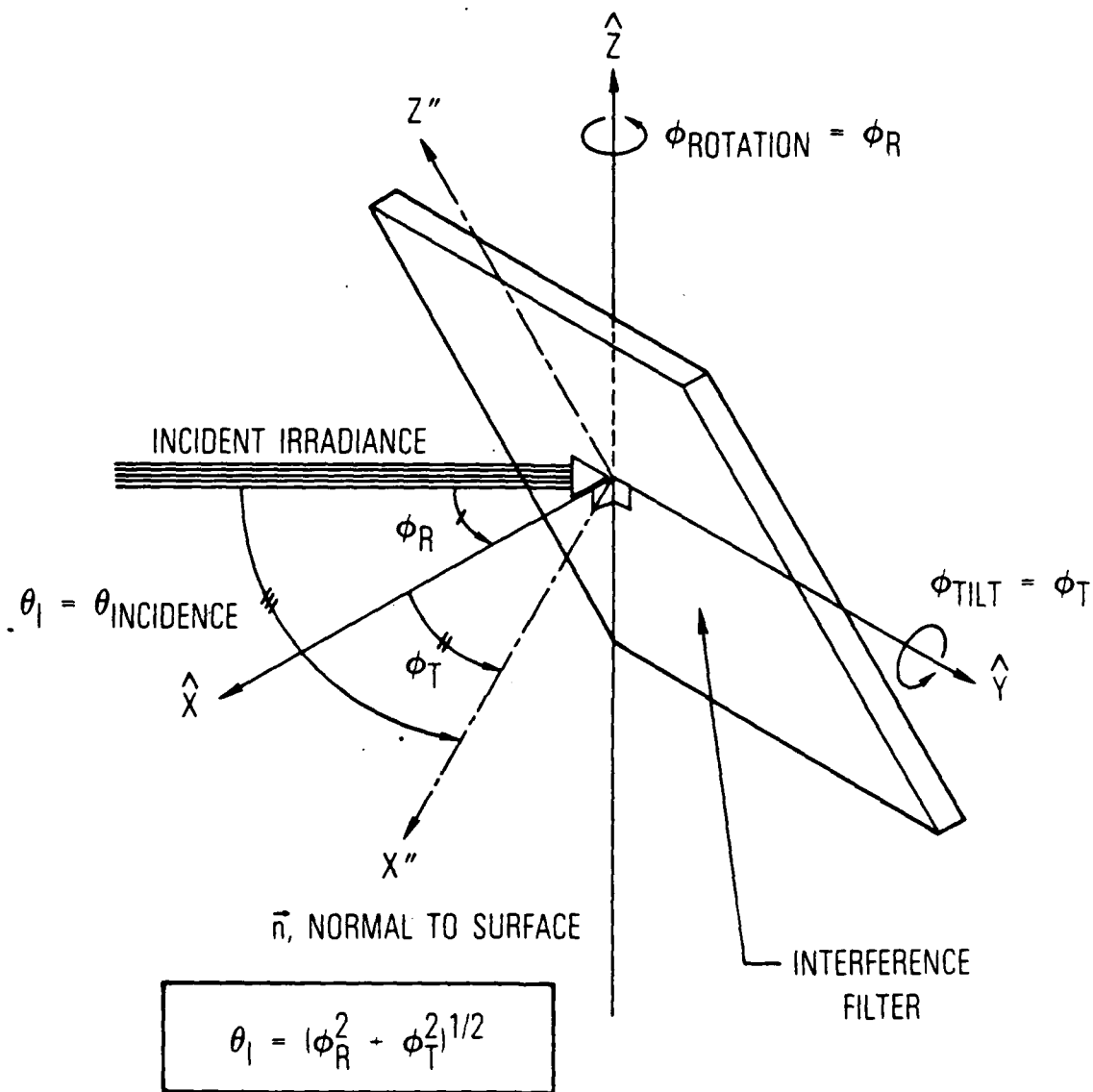


Fig. 1. Filter Angular Geometry for Dual-Planar Filter

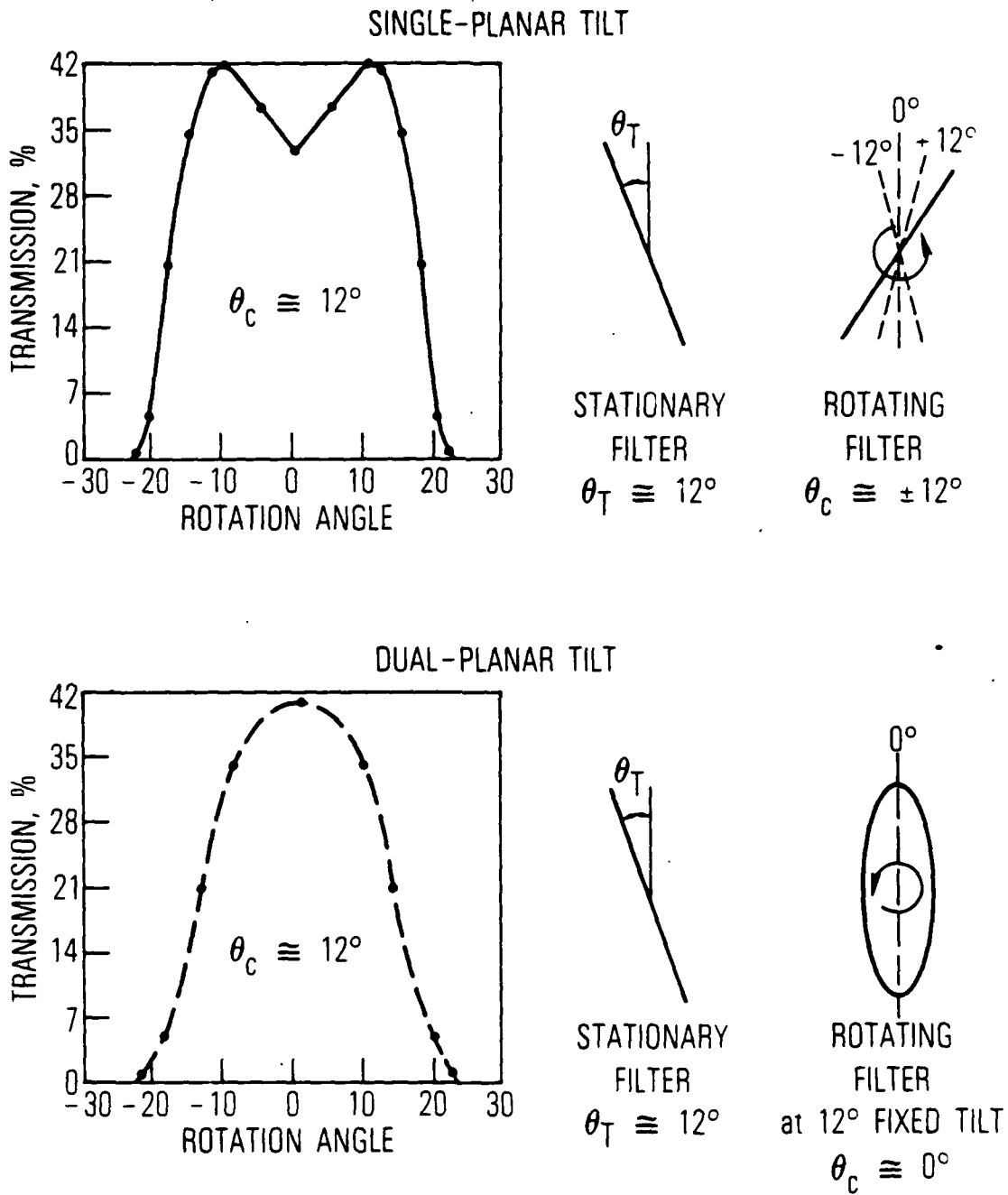


Fig. 2. Comparison between Single- and Dual-Planar Tilt with Identical Filters

III. DESIGN VERIFICATION

Design verification of this invention* was accomplished with three narrowband spectral filters selected from the current laboratory inventory. Specifically, a visible light and two similar midinfrared filters were used to demonstrate the spectral versatility of this shuttering method. Unless otherwise noted, all tilt angles discussed are measured with respect to the image plane of both the focusing optics and the image-sensing layer set up in the conventional manner, perpendicular to the optical axis.

The visible-light filter (Filter I) at 0° tilt has a 0.6338- μm center wavelength λ_0 , a 0.010- μm bandwidth $\Delta\lambda$, and a 67.7% peak transmission efficiency T_{eff} . Figure 3 plots the spectral transmission scans for this filter as it is tilted from 0 to 35°. Figure 4 shows how λ_0 , $\Delta\lambda$, and T_{eff} for Filter I change with increased angular tilt.

The two midinfrared filters (Filters II and III) have similar but not identical spectral transmission characteristics. At 0° tilt, Filter II has a λ_0 , $\Delta\lambda$, and T_{eff} of 3.460 μm , 0.11 μm , and 64.4%, respectively, whereas these parameters for Filter III are respectively 3.44 μm , 0.073 μm , and 69.6%. Figures 5 and 6, respectively, are the spectral transmission scans for Filters II and III as the filters are tilted from 0 to 38°. The changes in λ_0 , $\Delta\lambda$, and T_{eff} caused by increased angular tilting of Filters II and III are shown in Figs. 7 and 8, respectively.

In all spectral shutter designs considered here, the moving filters are operated at 30 revolutions per second. This rotational rate can be synchronized with the frame rate of conventional television cameras and is well within state-of-the-art motor design. The refractive optics used in all the following examples are assumed to have a 2.0-in.-diam aperture and a 1-in.-diam image plane.

*Patent pending.

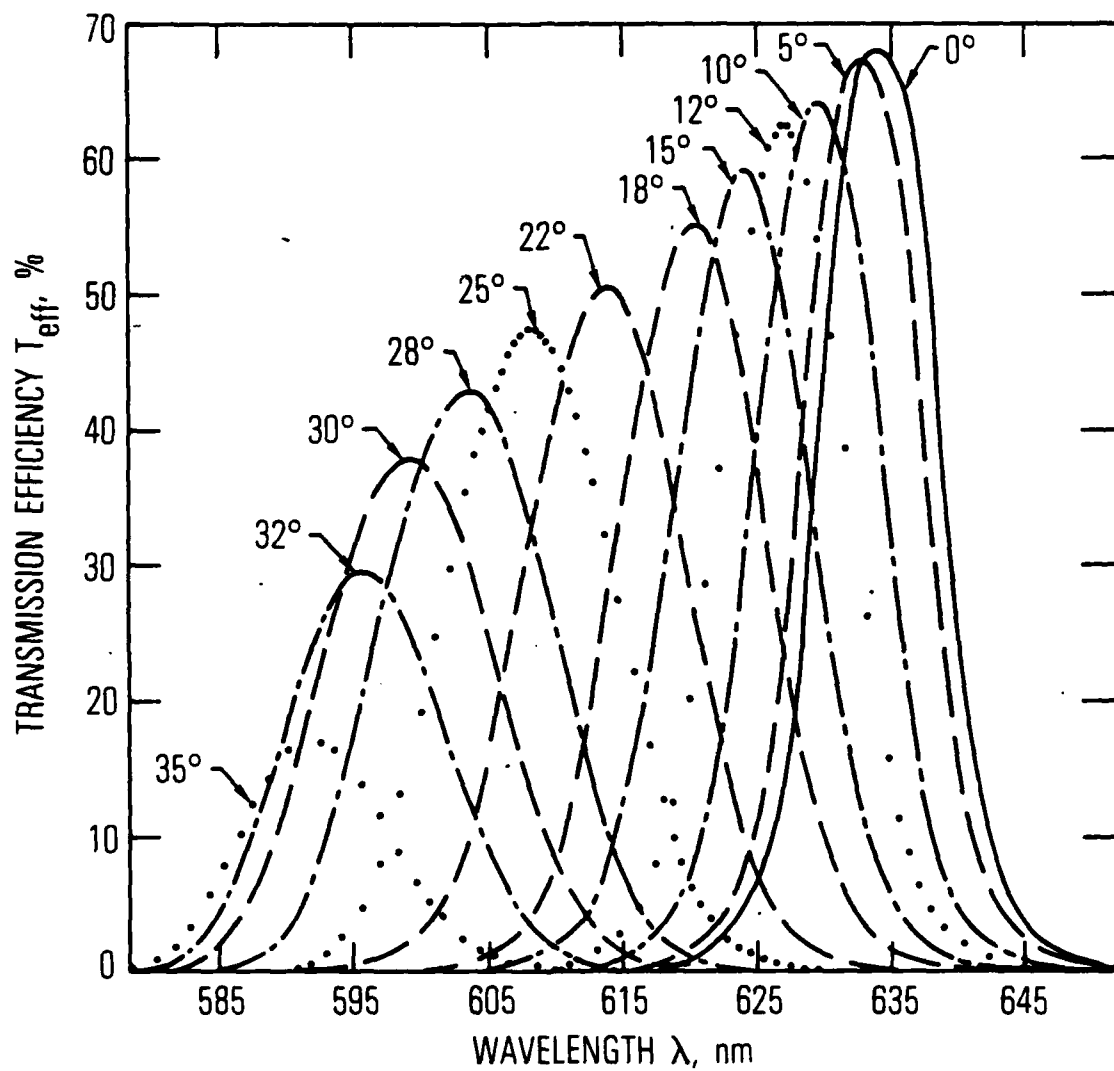


Fig. 3. Filter I Transmission Scans for 0 to 35° Tilt Angles θ_T

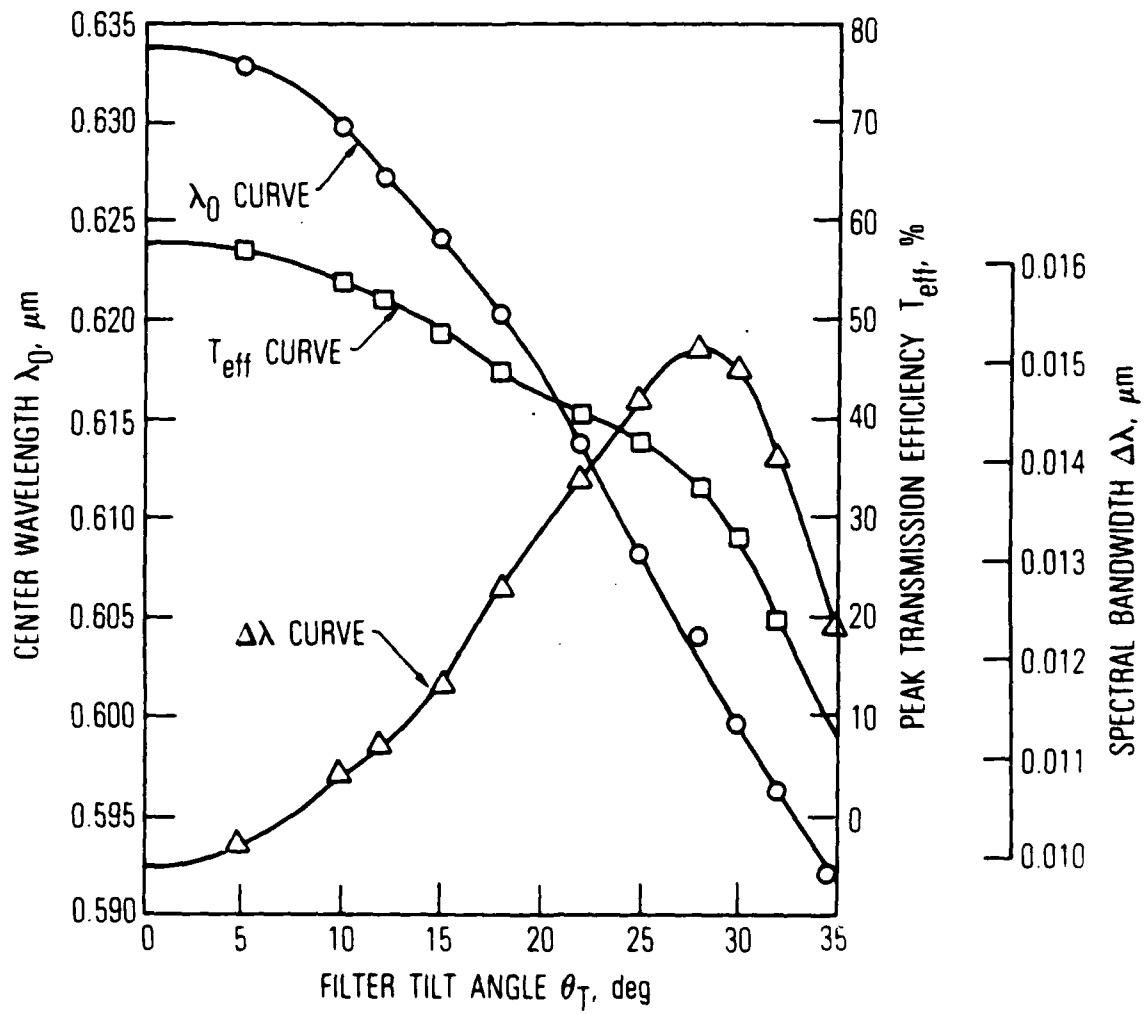


Fig. 4 Filter I Bandpass Parameters (λ_0 , T_{eff} , and $\Delta\lambda$) as a Function of Angular Tilt θ_T

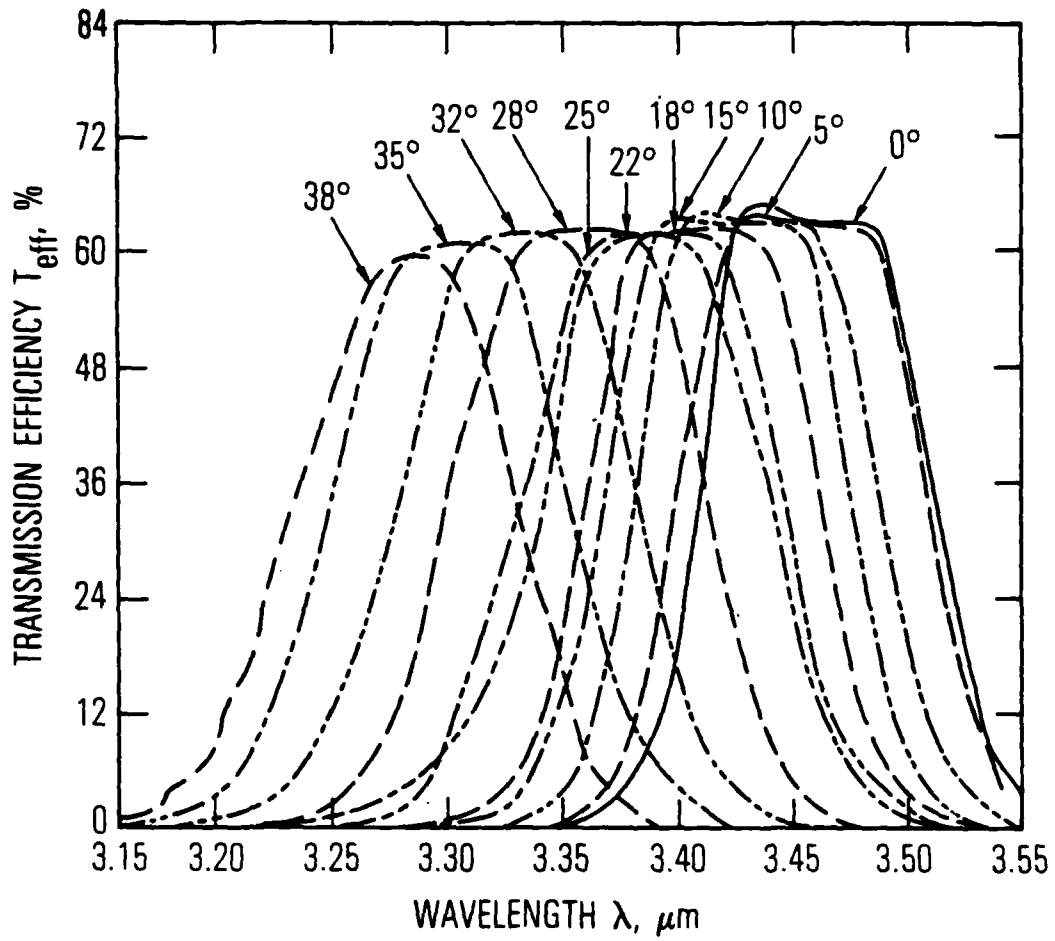


Fig. 5. Transmission Scans for 0 to 38° Tilt Angles θ_T

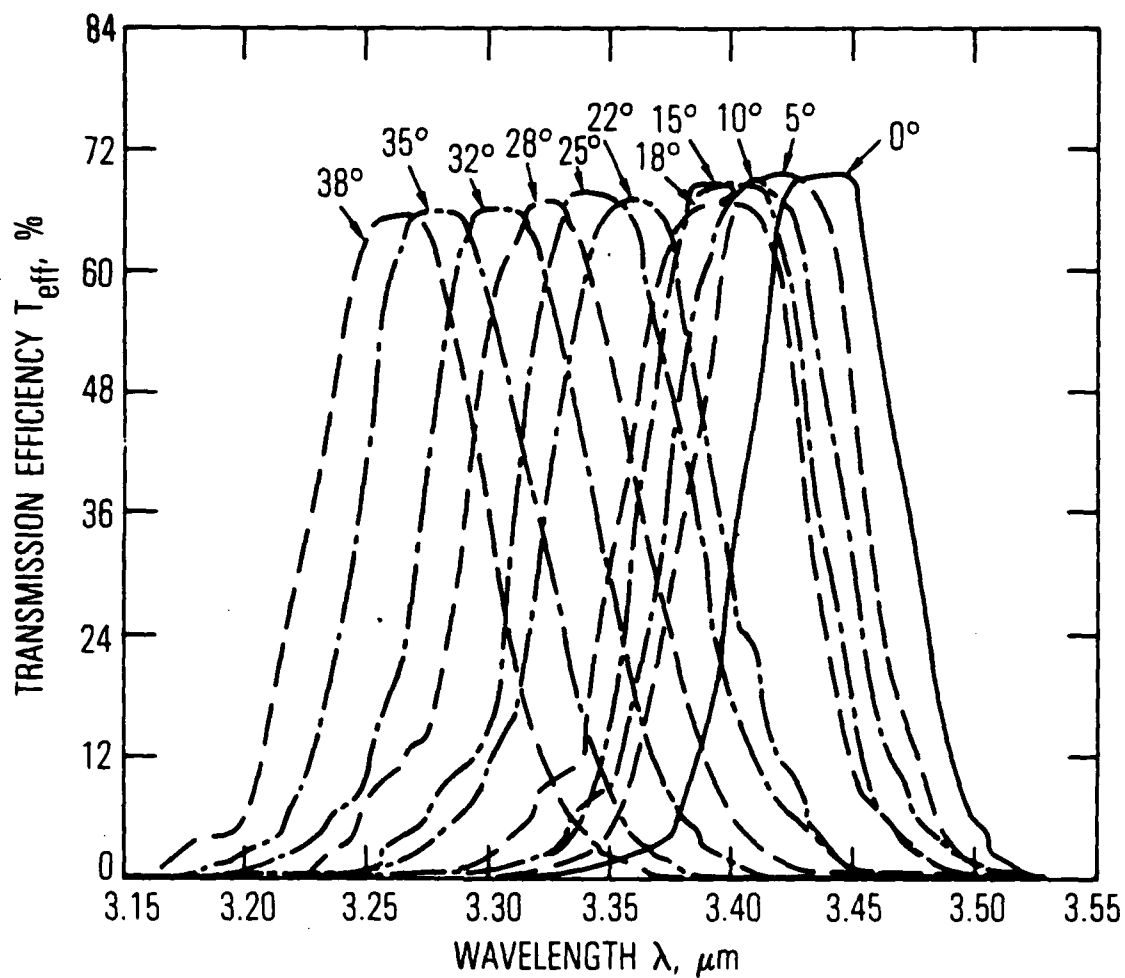


Fig. 6. Filter III Transmission Scans for 0 to 38° Tilt Angles θ_T

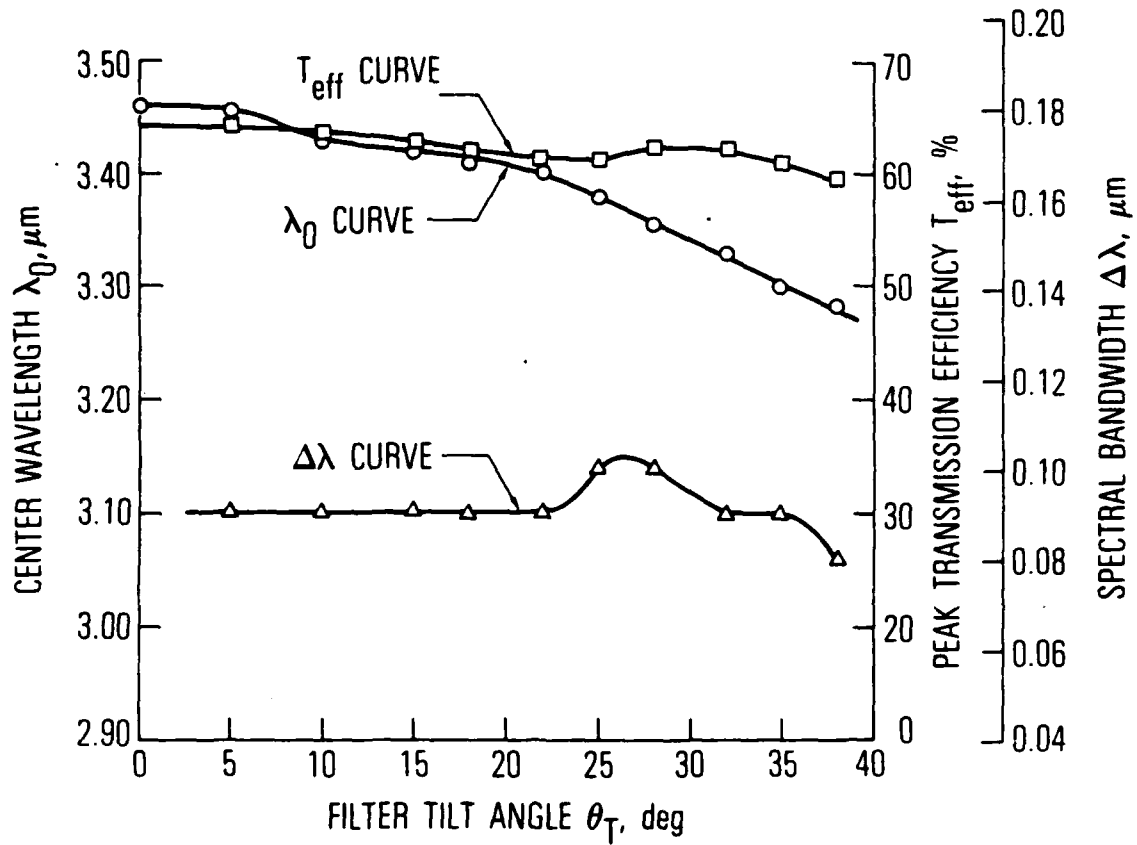


Fig. 7. Filter II Bandpass Parameters (λ_0 , T_{eff} , and $\Delta\lambda$) as a Function of Angular Tilt θ_T

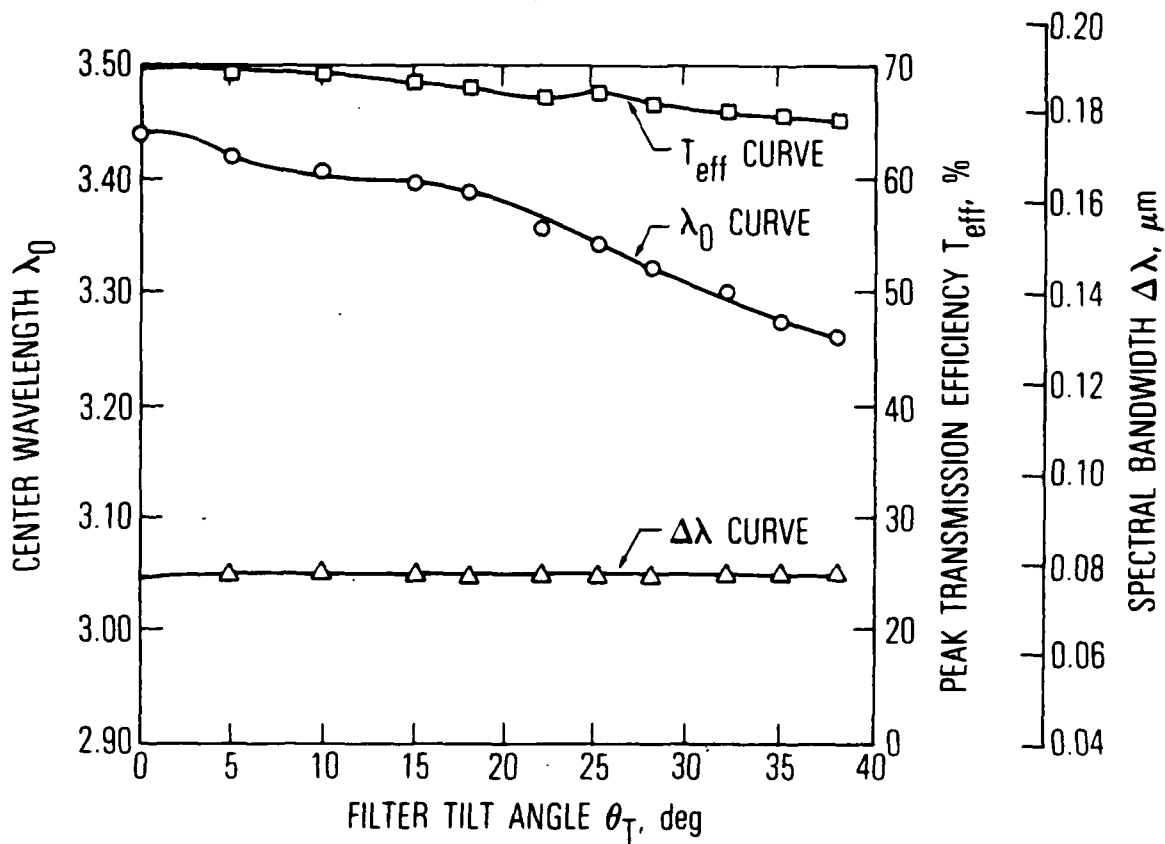


Fig. 8. Filter III Bandpass Parameters (λ_0 , T_{eff} , and $\Delta\lambda$) as a Function of Angular Tilt θ_T

The simplest version, Spectral Shutter Design A (see Fig. 9), consists of two infrared bandpass filters installed in front of the camera optics, with one filter stationary and the other revolving. For this design configuration, open shutter occurs at θ_c when $|\theta_T|$ is the same for both filters. These filters should have similar bandpass transmission characteristics over the 0 to 45° tilt range and should satisfy specific spectral response requirements of the camera system at θ_c . To increase opening and closing speeds for Shutter Design A, θ_c should occur at the knee of the curve of wavelength versus $|\theta_T|$. The baffling shown on the rotating filter in Fig. 9 provides necessary additional optical blockage when the filter is outside the coincident-angle range and does not completely cover the lens aperture. When Filter I is used in Design A (A-I), Fig. 10 graphs the composite transmission profiles as a function of θ_T during the open-shutter period. As seen in this example, maximum peak transmission (open shutter) is 30.7% at 0.6210 μm for $\theta_T = 18^\circ$.

Although Spectral Shutter Design A clearly demonstrates the operational principle, it is not the optimum repetitive shuttering configuration for use with a conventional television camera. During each filter revolution, the four open-shutter periods occur at alternating angular displacement values. Consequently, a more complex electromechanical design would be required to have one "snap-shot" image per picture frame at conventional television rates. Also, since the filter wavelength changes are more rapid for $|\theta_T| > |\theta_c|$ than they are for $|\theta_T| < |\theta_c|$, the time differential between open and closed aperture is longer and less sharply defined on one side of the shutter transmission curve. Using Design A-I, the curve of shutter transmission versus angular displacement for a single line is plotted in Fig. 11. Unfortunately, this A-I spectral shutter does not provide sufficient transmission rejection ($T_{\text{eff}} > 10\%$) in the rotational sector where $|\theta_T| < |\theta_c|$.

The design problems discussed in the previous paragraph can be eliminated by setting the rotating filter at a fixed tilt angle in one plane and then revolving the filter in the orthogonal plane. Also, to increase T_{eff} and more sharply define t_{os} , the stationary filter can be designed with a spectral bandpass equivalent to the revolving filter at θ_c and installed parallel to

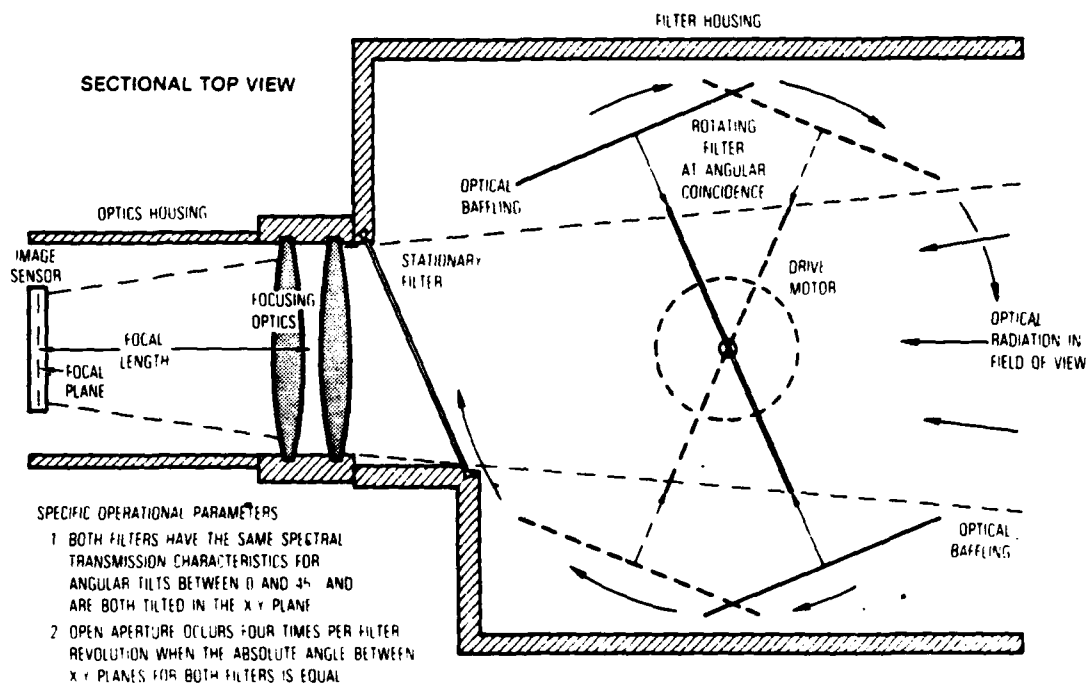


Fig. 9. Spectral Shutter Design A, a Stationary and Rotational Filter Combination Using Single-Planar Tilt at the Optical Aperture

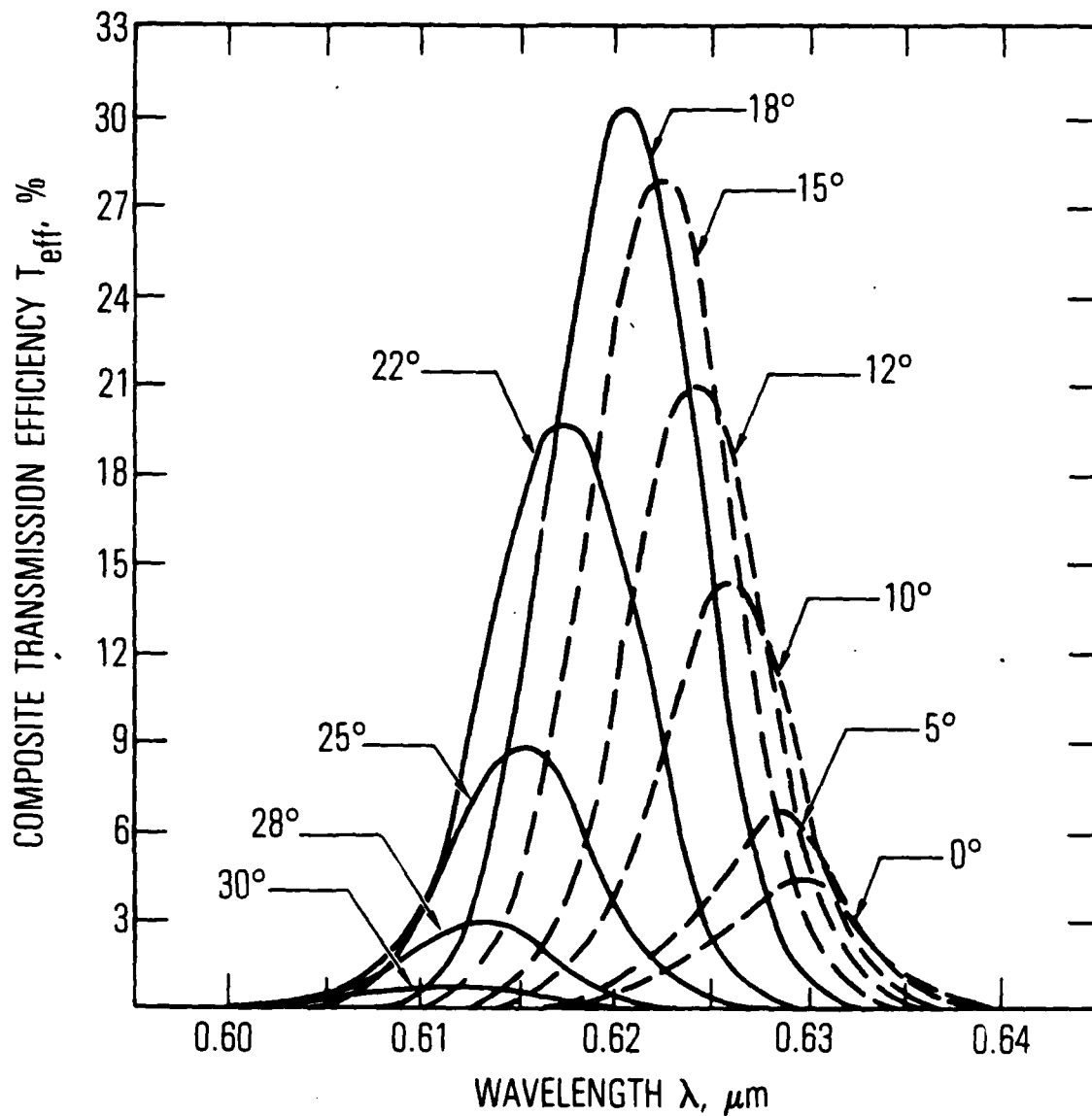


Fig. 10. Spectral Shutter Design A with Filter I Composite Transmission Profiles for Filter Angular Displacements

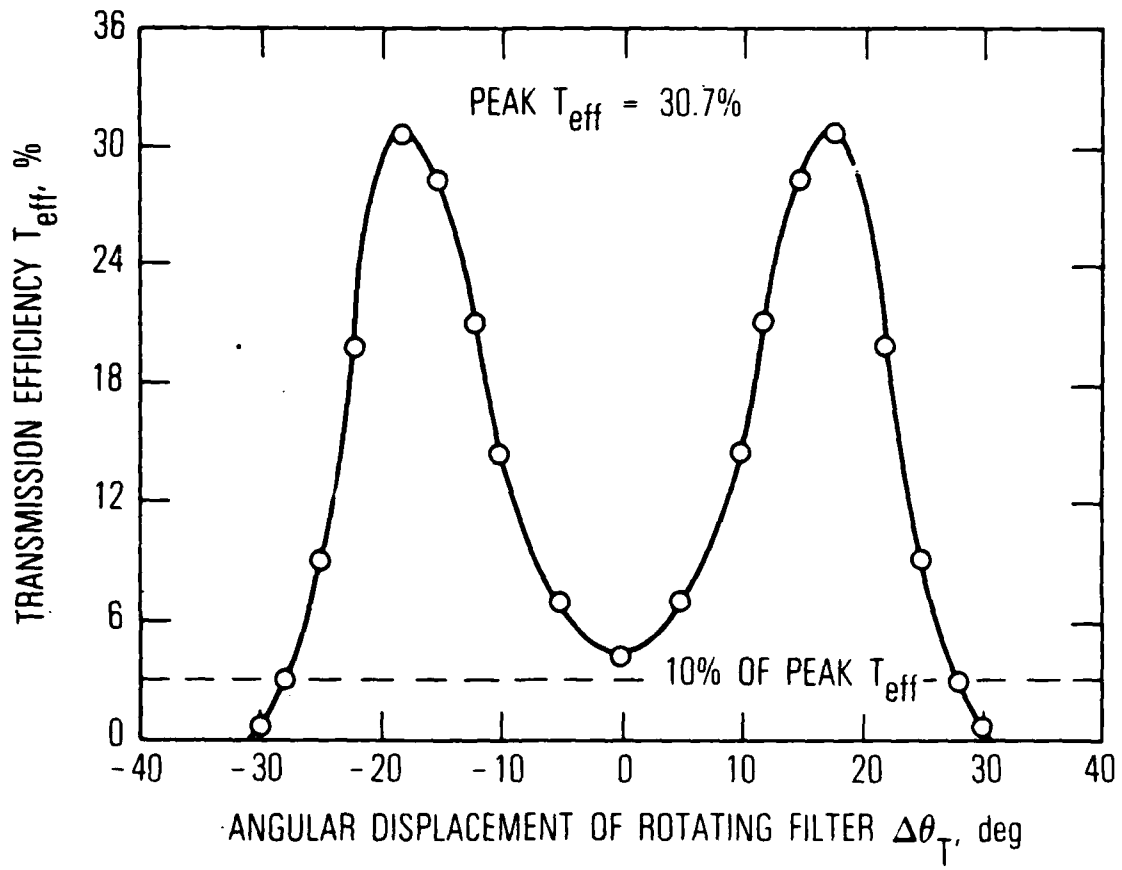


Fig. 11. Spectral Shutter Design A with Filter I Composite Transmission Efficiency versus Tilt Angle θ_T

the image plane (i.e., at 0° tilt). Spectral Shutter Design B, shown in Fig. 12, diagrams this approach for a pair of filters where the revolving filter is initially tilted in the y-z plane and Θ_c occurs only when the rotational tilt in the x-z plane is zero. Under these operating conditions, open shutter occurs twice per revolution, where the rotating filter has a minimum dual-planar tilt angle equal to the fixed Θ_T value in the y-z plane.

Figure 13 graphs the transmission scans for Filters I and I' at 12° and 0° tilt, respectively. Filter I' is synthesized to produce the same coincident center wavelength as the setup in Design A-I. When Filters I and I' are used in Design B (B-I/I'), Fig. 14 plots the composite transmission profiles for B-I/I' as a function of Θ_T during open-shutter times. As seen here, peak transmission efficiency is 41.2% at $0.628 \mu\text{m}$ for Θ_T (y-z, x-z) = 12° and 0° . Using the transmission profiles in Fig. 14, shutter transmission versus angular displacement is plotted in Fig. 15. The t_{os} derived from this graph are 3.1 and 3.6 ms for single-line and uniformly continuous irradiance, respectively.

Spectral Shutter Design C, shown in Fig. 16, has the same operational parameters as Design B, except that its stationary filter is installed immediately in front of the image plane. This configuration has the advantage that the stationary filter can be reduced in size from aperture to image-plane diameter. In Fig. 16, the stationary-filter diameter is decreased from 2.25 to 1.00 in. by relocation. However, Design C cannot always be implemented, because in some image systems it is either very difficult or not feasible to install the filter in such close proximity to the focal plane. Also, in some cases where spectral bandpass must be changed several times, each replacement and/or adjustment of the stationary filter in Shutter Design C could make operating procedures significantly more complex.

Simultaneous rotation of both bandpass filters can produce faster shutter speeds than are realizable with the three previous designs. Such an approach is exemplified by Spectral Shutter Design D (see Fig. 17), where a single shaft rotates the assembly holding both filters. Since this diagram assumes that both filters have the same spectral transmission characteristics, each

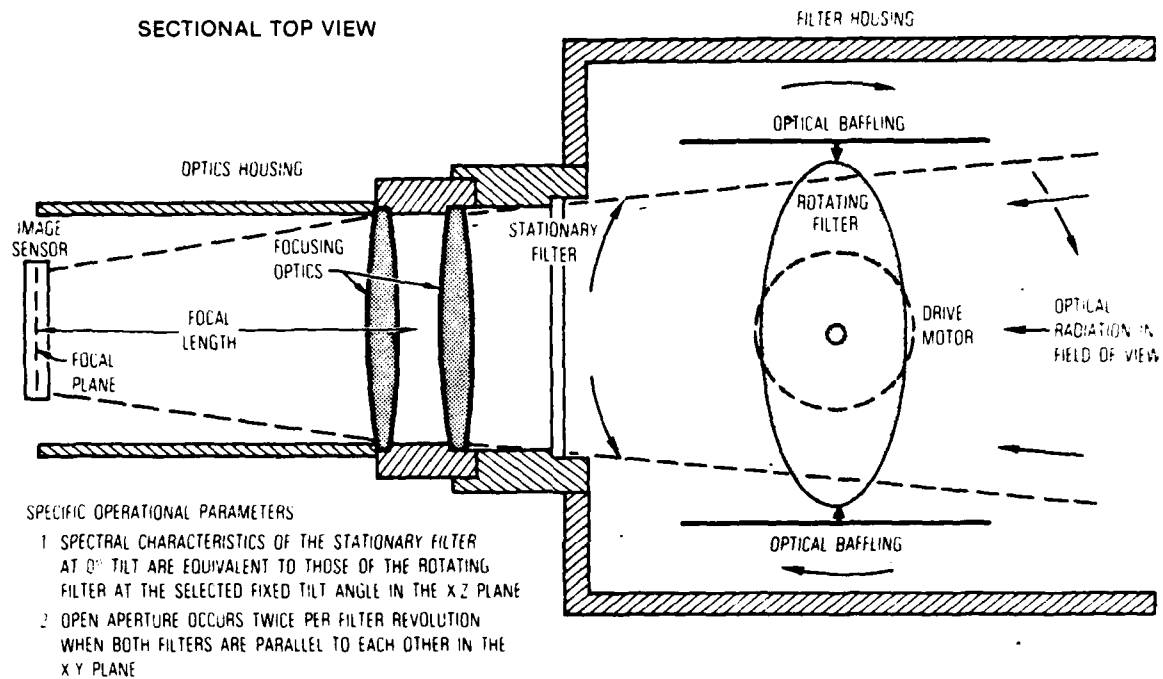


Fig. 12. Spectral Shutter Design B, a Stationary and Rotational Filter Combination Using Dual-Planar Tilt at the Optical Aperture

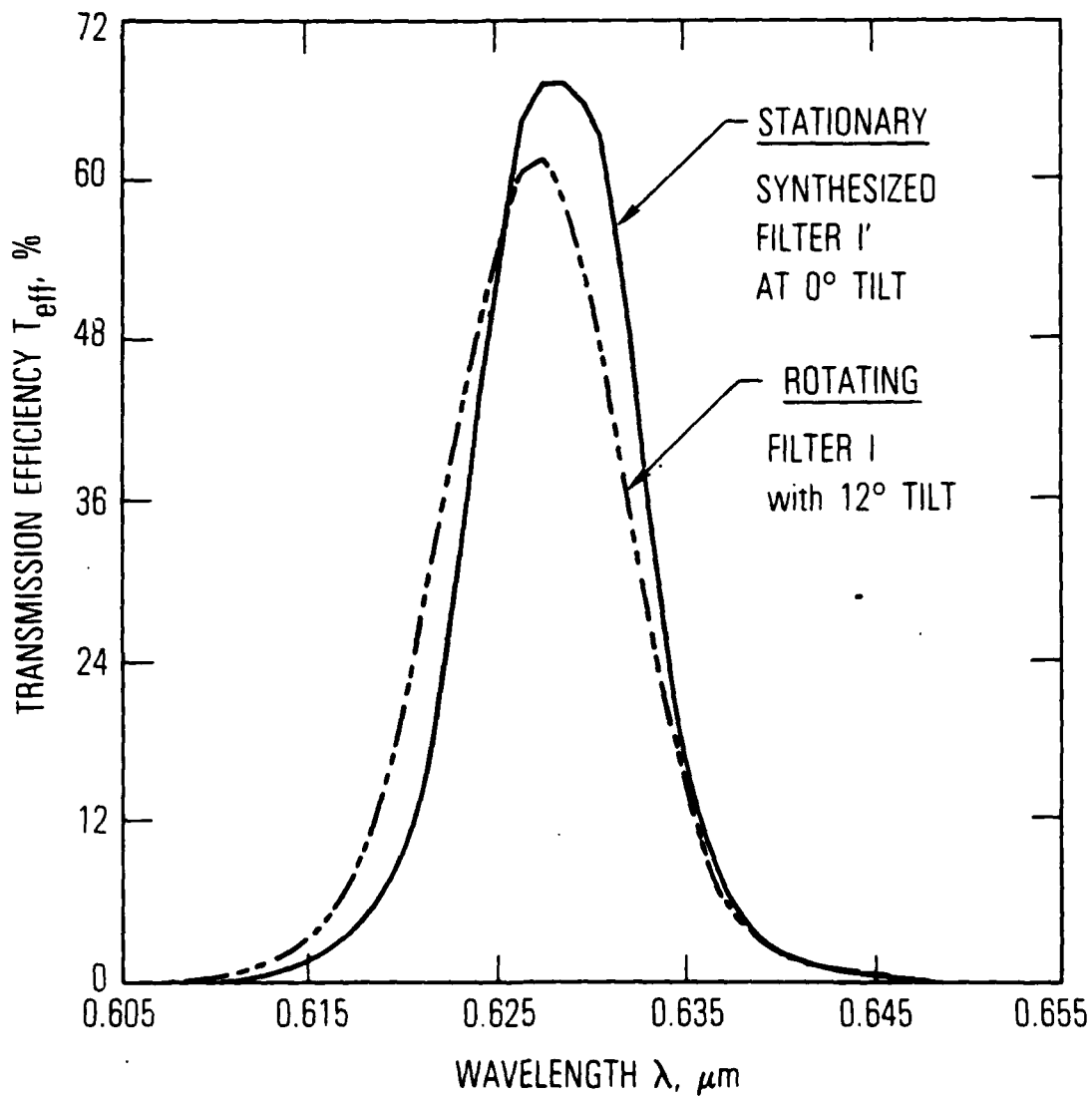


Fig. 13. Transmission Scans for Filters I and I' at Angular Coincidence

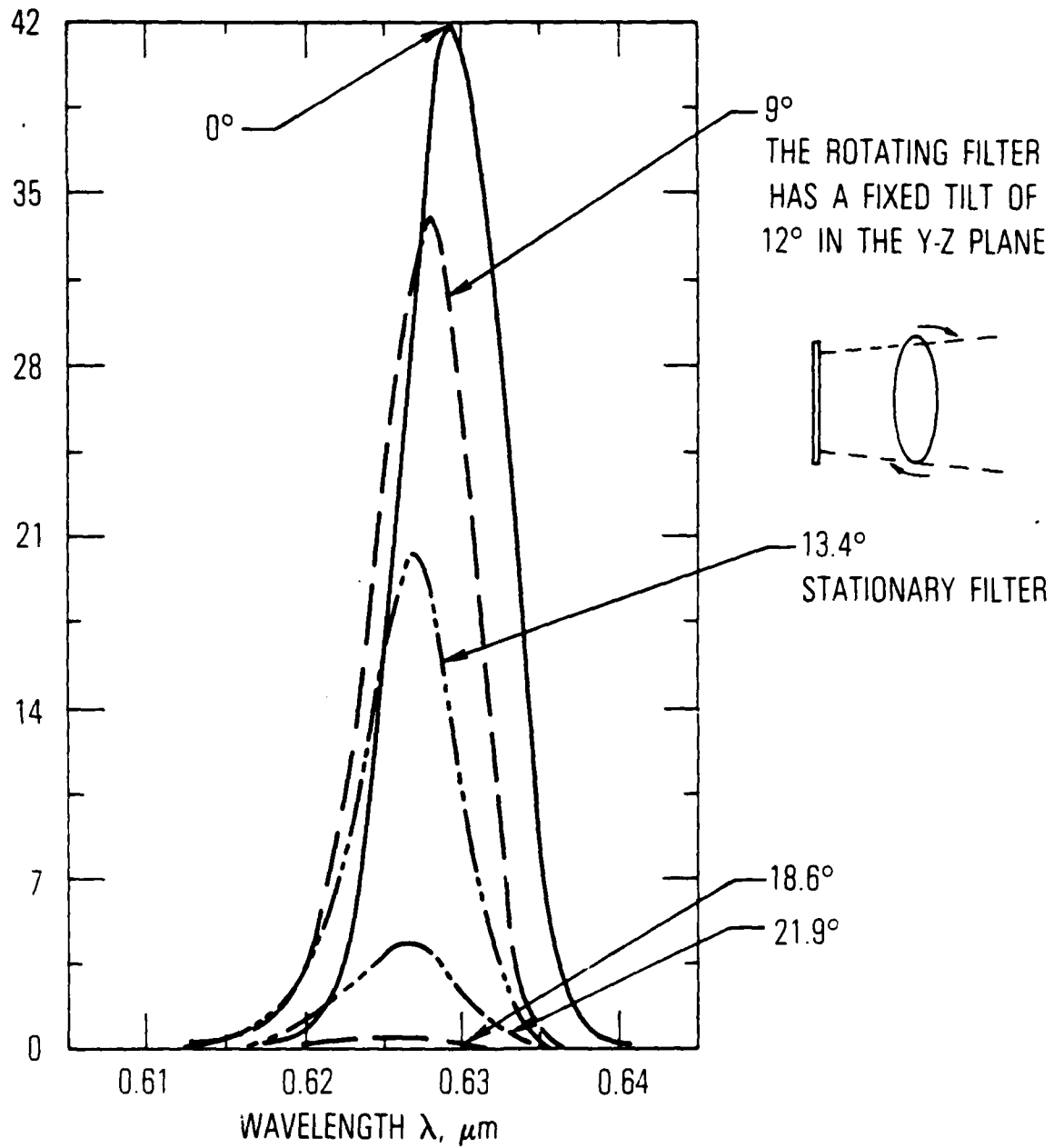


Fig. 14. Spectral Shutter Design B with Filters I and I' Composite Transmission Profiles for Filter Angular Displacement

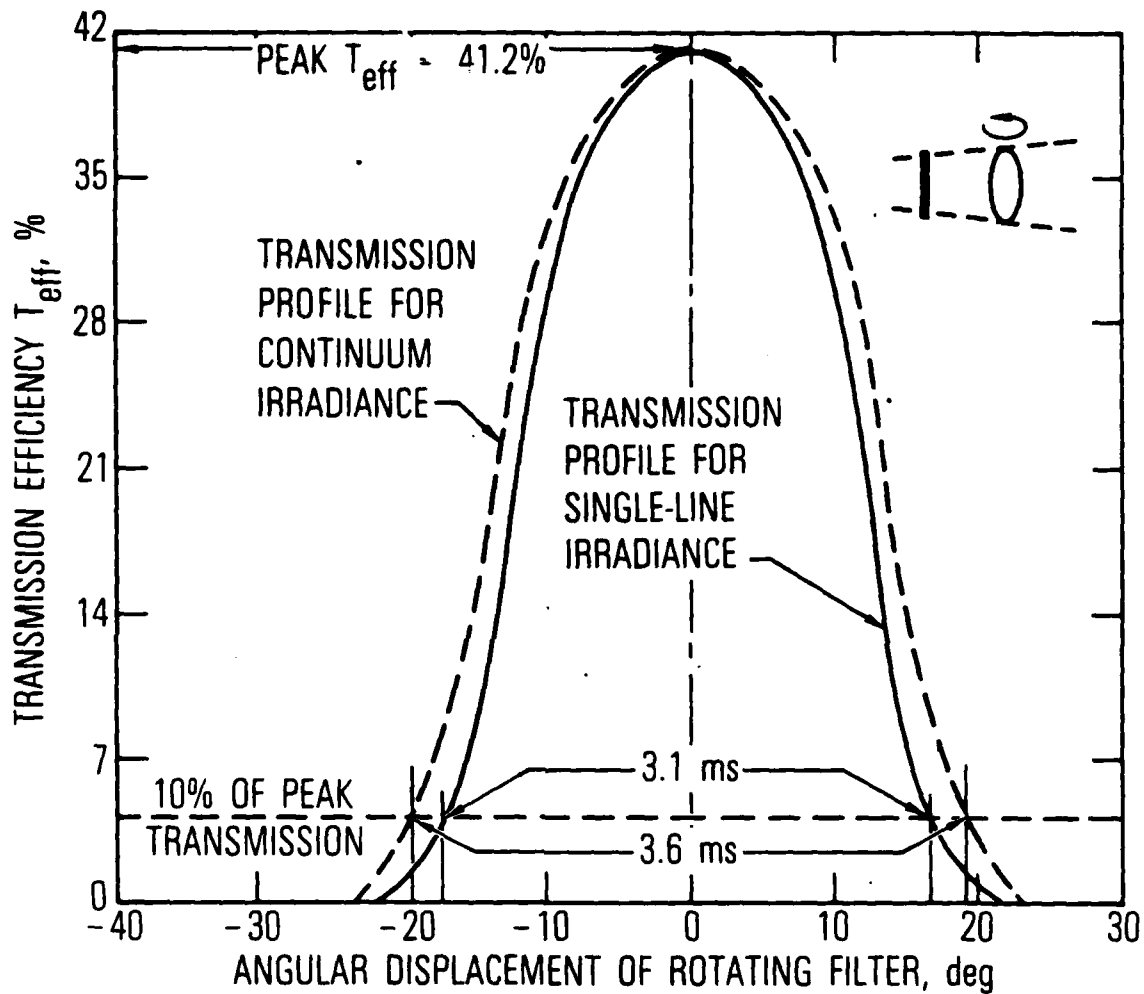


Fig. 15. Spectral Shutter Design B with Filter I Composite Transmission Efficiency T_{eff} versus Tilt Angle θ_T

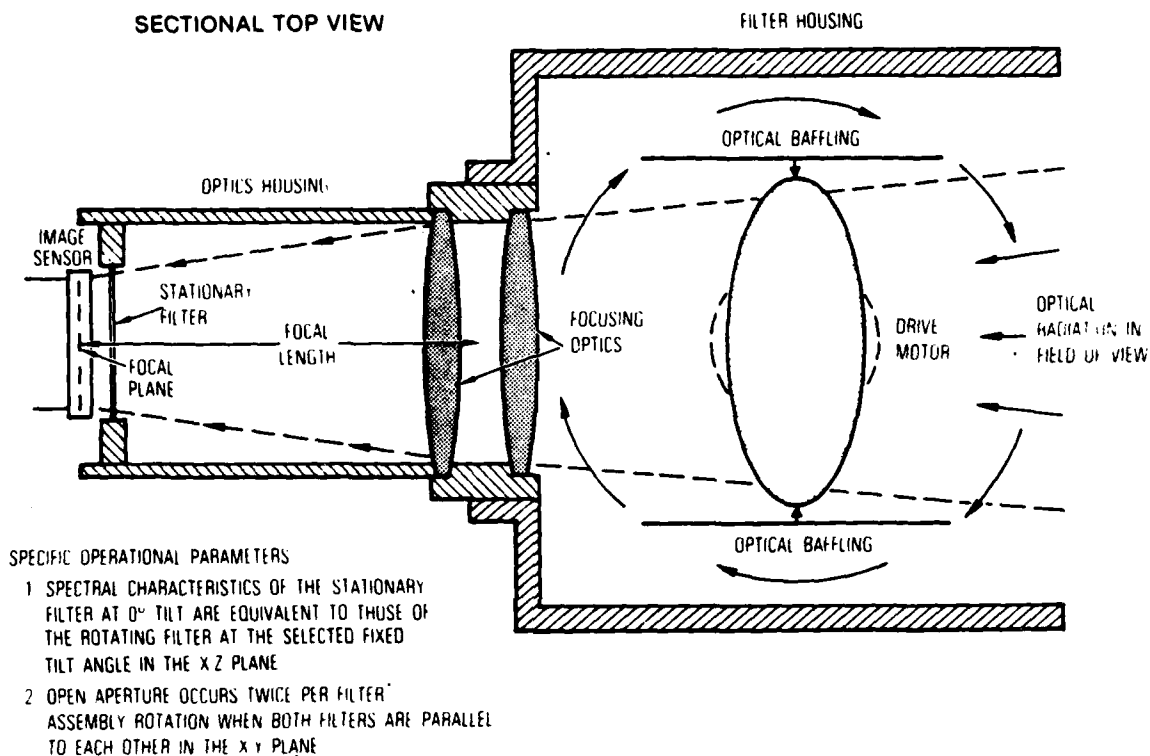


Fig. 16. Spectral Shutter Design C, a Stationary Filter near the Focal Plane and a Rotating Filter with Dual-Planar Tilt at the Optical Aperture

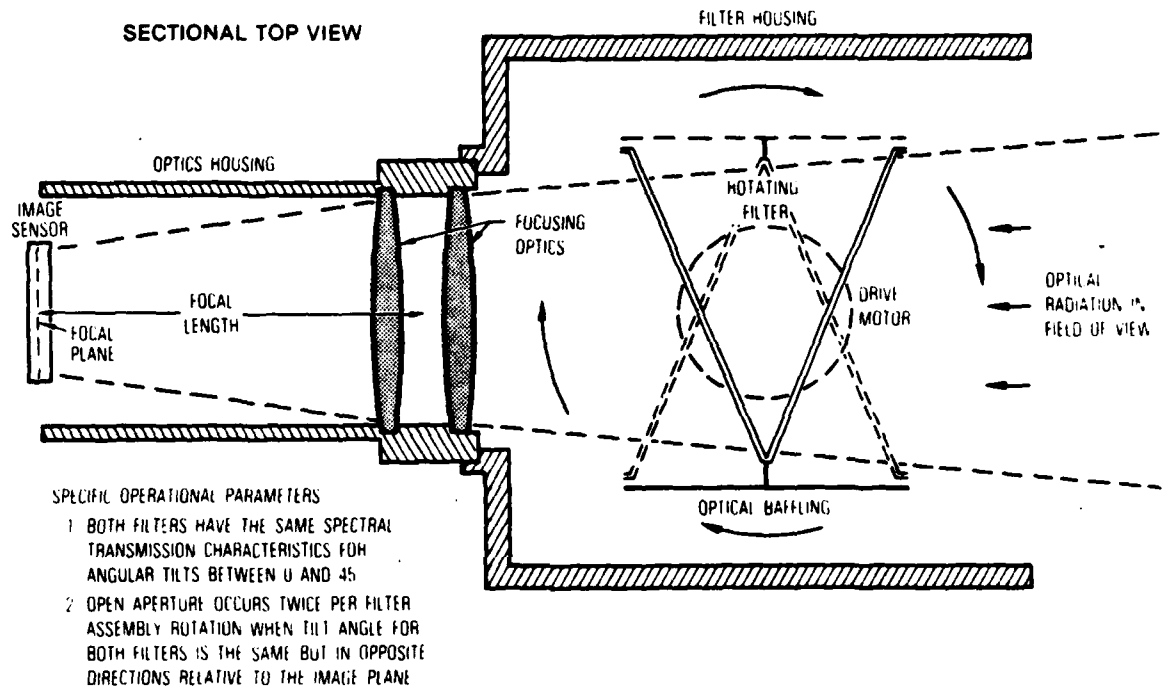


Fig. 17. Spectral Shutter Design D, a Double Rotational Filter Combination Using Single-Planar Tilt at the Optical Aperture

has the same angular tilt relative to the image plane, but in opposite directions. Open aperture occurs twice during every revolution of the two-filter assembly with a 180° separation. Because both filters are rotated as a unit instead of individually, the open-shutter time is cut in half.

When two Filter I' are used in Design D, Fig. 18 shows the composite transmission profiles for selected Θ_T values during the shuttering period. Using the transmission profiles in Fig. 18, shutter transmission versus angular displacement is plotted in Fig. 19. The derived t_{OS} for single-line and uniformly continuous irradiance are measured to be 1.39 and 1.48 ms, respectively.

When Filters II and III are used in Design D, Fig. 20 shows the composite transmission profiles for selected Θ_T values during the shuttering period. Using the transmission profiles in Fig. 20, shutter transmission versus angular displacement is plotted in Fig. 21. The derived t_{OS} for single-line and uniformly continuous irradiance are measured to be 1.8 ms under both conditions.

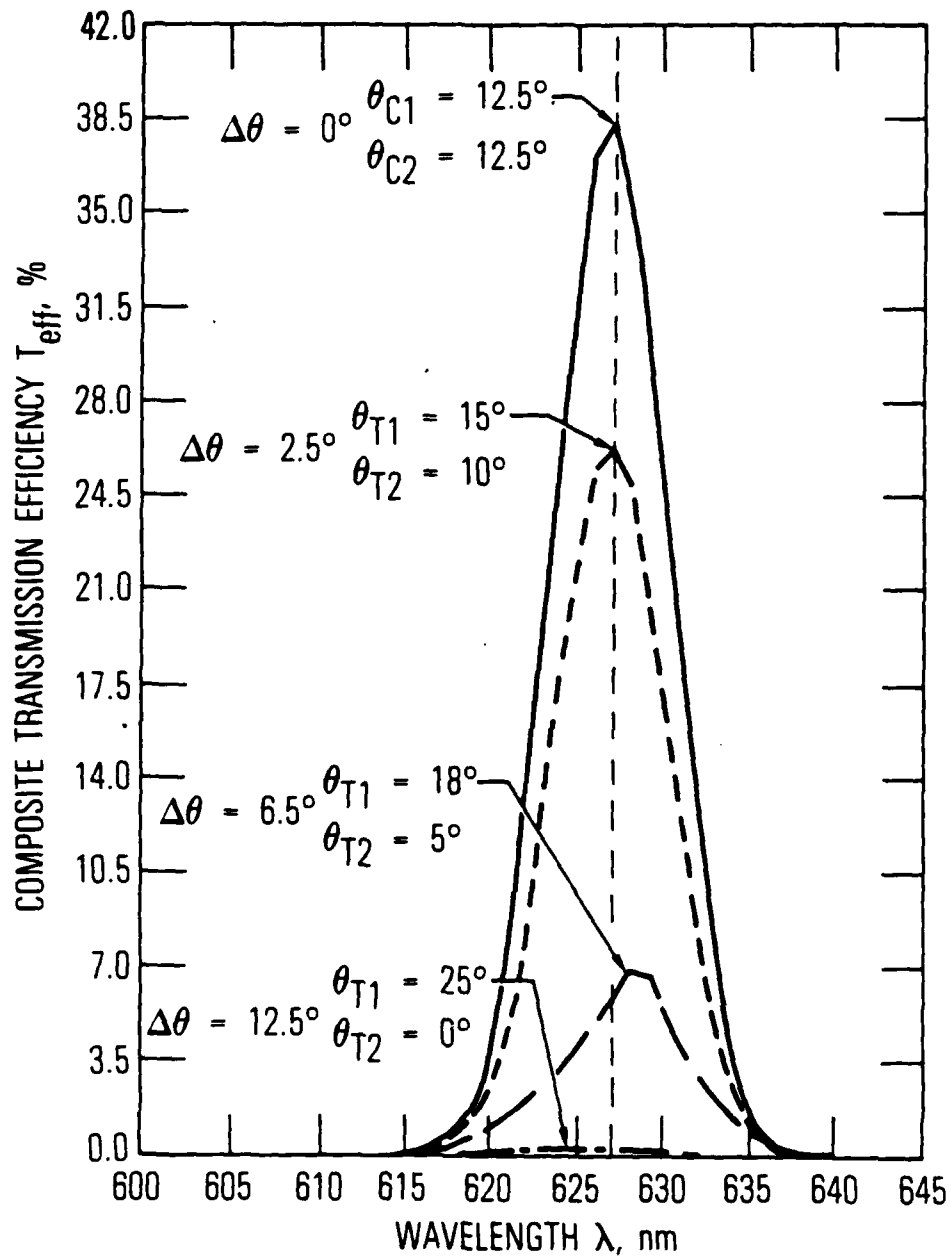


Fig. 18. Spectral Shutter Design D with Filter I Composite Transmission Profiles for Filter Angular Displacements

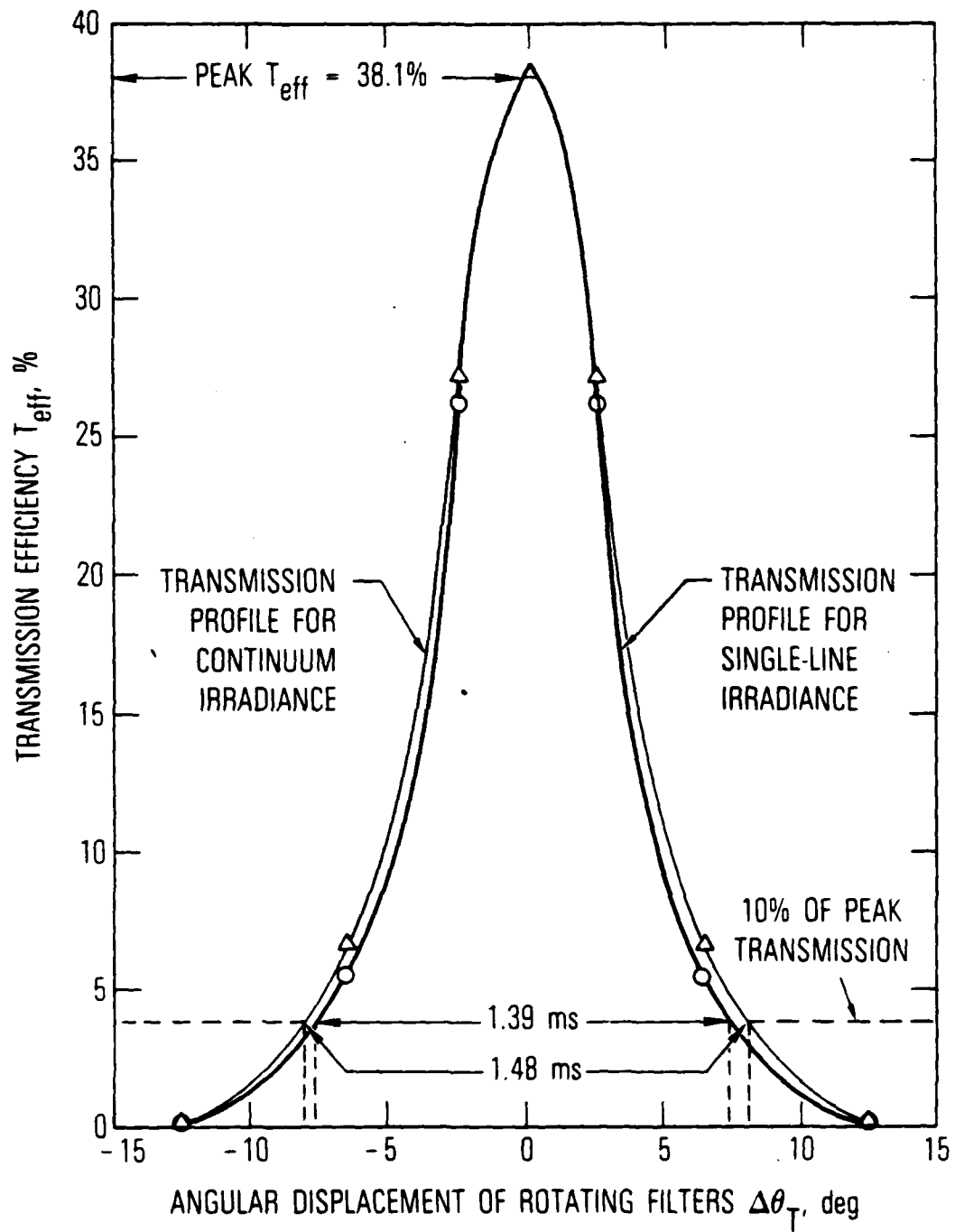


Fig. 19. Spectral Shutter Design D with Filter I Composite Transmission Efficiency T_{eff} versus Tilt Angle θ_T

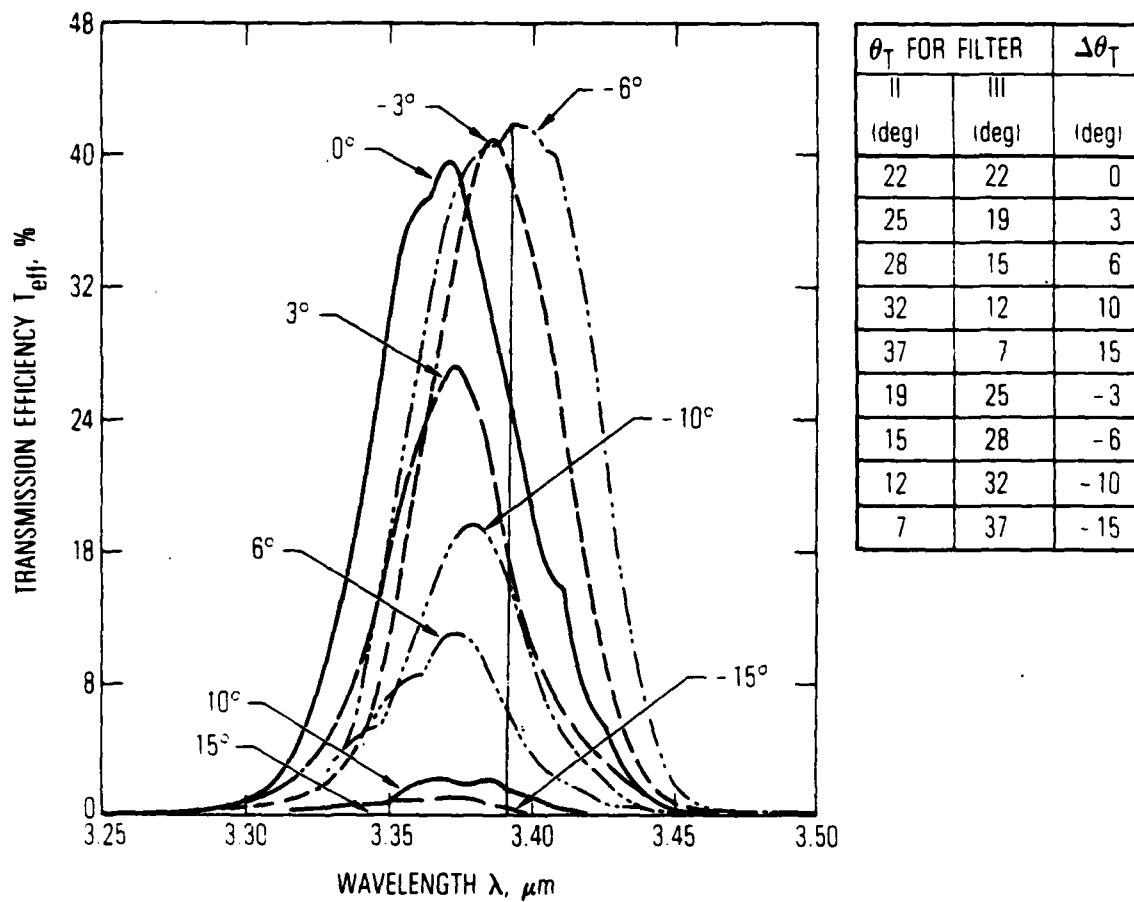


Fig. 20. Spectral Shutter Design D with Filters II and III Composite Transmission Profiles for Filter Angular Displacements

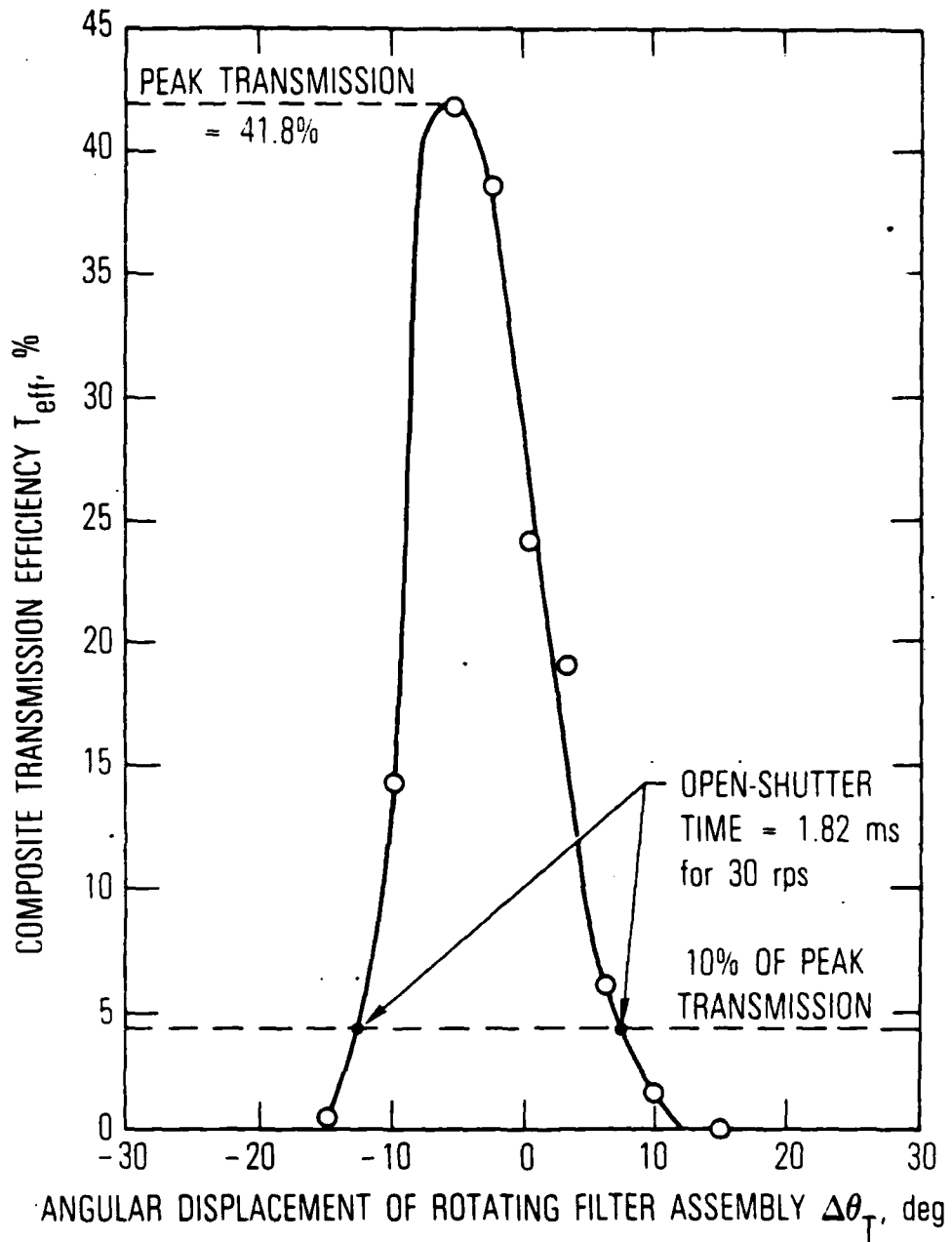


Fig. 21. Spectral Shutter Design D with Filters II and III Composite Transmission Efficiency T_{eff} versus Tilt Angle θ_T

IV. CONCLUSIONS

The spectral shuttering mechanism described in this report can repetitively provide open-shutter times in the 1 to 4-ms range at television rates. The performance required from all mechanical and optical components in this device is attainable with the current state of the art. If, however, the narrowband filters were tailored specifically for this purpose, further improvement in shutter speed, transmission efficiency, and spectral characteristics could probably be realized. For some applications the continual filter rotation could be replaced by the "butterfly motion" derived from a stepper motor or an equivalent mechanical linkage. In this manner faster shutter speeds could be obtained, but maximum attainable repetition rate would be less than realizable with conventional synchronous motors.

This new optomechanical technique for shutter viewing in a narrow spectral region (i.e., one having a bandwidth less than $0.1 \mu\text{m}$) has unique features not readily available in conventional electromechanical shutters. These performance advantages include the capability to provide (1) "snap-shot" imagery that always encompasses the entire field of view, (2) self-contained spectral selectivity for focused signal irradiance, (3) greater transmission efficiency during the open-shutter times, and (4) adaptability to a wider variety of optical systems.

To obtain blur-free video data of fast-moving images, the spectral filter technique is a more reliable shutter mechanism than a rotating chopper wheel. The two-filter configurations monitor the entire field of view during open aperture, but the chopper wheel method sweeps across the image plane in such a way that fully open aperture occurs at only one instance of time. Therefore, since the chopper wheel is continually masking different segments of the focal plane, video signals from rapidly moving targets and radiant intensity levels vary with both target position and movement on the image plane during open-aperture sweep times.

Because the shuttering action is accomplished by varying spectral characteristics of one or two bandpass filters, scene irradiance at the focal plane has a higher wavelength selectivity than is exhibited by either filter individually. As a consequence, integration of both signal and background irradiance is confined to open-shutter times and this narrowed spectral band. Specifically, both these features could be useful in the design of an image system for viewing pulsed laser energy. For such an application, camera observations could be synchronized with the laser pulse rate, thereby limiting signal irradiance to the laser wavelength while simultaneously using background irradiance in the field of view.

Typically, many video cameras with high-speed shuttering obtain submillisecond and microsecond speeds with a complex lens action that uses several optical elements. These currently available shutters are significantly less efficient in the transmission of signal irradiance than is this new dual-filter configuration. In addition, the electromechanical approaches must be tailored individually for a specific optical application.

If the mechanical chopping is performed where image irradiance converges to a point in front of the focal plane, submillisecond shuttering can be achieved with long-focal-length optics. However, this approach is not compatible with short-focal-length, high-speed optics because the location, alignment, and size of the chopper aperture become exceedingly critical. Any slight change in open-aperture location resulting from the high chopper rates will significantly reduce image irradiance and produce nonuniformities in the scene imagery. Since this spectral shutter mechanism is a self-contained device installed immediately in front of the optical aperture, alignment requirements are considerably less critical and there is no dependence on the selected optical f-number.

Present operational limitations associated with this fast shutter device are related to spectral bandwidth, filter size, and optical transmission efficiency.

This shutter mechanism is based on the phenomenon that the spectral transmission of a bandpass filter progressively moves to lower wavelengths as angular tilt between filter and image plane departs from parallel orientation. This effect is very pronounced in narrow-bandpass filters having bandwidths of 0.1 μm or less, but for wider bandwidths angular positioning is less significant. Therefore, this shuttering technique is only applicable to image systems where target irradiance can be restricted to small bandwidths. In many applications, however, this requirement does not severely inhibit system performance, because the narrow spectral band (1) reduces background irradiance in the field of view, (2) increases image contrast between target and background irradiance, and (3) is well suited for monitoring line spectra energy from laser targets.

When an imaging system is required to operate at maximum collecting power, the revolving filter assembly must not "aperture-stop" the optics. To meet this criterion, filter size should be sufficiently large to cover the entire optical field of view during the coincident tilt-angle phases. For the 2.0-in.-diam, f/1.2 optics used in all previous examples, the revolving filters are required to be at least 3.0 in. in diameter. As the optical aperture increases, it becomes progressively more difficult and expensive to fabricate the larger high-quality bandpass filters necessary for this shuttering technique.

When this shutter mechanism is in the open-aperture position, signal irradiance is transmitted through both bandpass filters, at least one of which is at a significant tilt angle. As a result, shutter transmission efficiency is at least 50% less than would be obtained through a narrowband filter parallel to the image plane.

In summary, this new rotating filter technique produces a fast and reliable shutter mechanism applicable to a wide range of detection and imaging systems. This device is uniquely qualified to provide high-speed framing for signal irradiances in a narrow spectral bandpass. Precise open-shutter times in the submillisecond range can be achieved at repetition rates that are limited only by motor speed. For a rotating chopper wheel to attain

equivalent shutter performance would be a difficult mechanical problem requiring a state-of-the-art motor design. The rotating filter configuration affords the additional features of increased background rejection and a more sharply defined time period for the open-aperture condition.

REFERENCES

1. Cross, E. F., M. A. Kwok, and D. C. Jonuska, "Method and Apparatus for Effecting Multiple Spectral Wavelength Imaging with Infrared Television," United States Patent 4,064,535 (20 December 1977).
2. "Effects of the Variation of Angle of Incidence and Temperature on Infrared Filter Characteristics," Optical Coating Laboratory, Inc. (May 1967).

LABORATORY OPERATIONS

The Laboratory Operations of The Aerospace Corporation is conducting experimental and theoretical investigations necessary for the evaluation and application of scientific advances to new military space systems. Versatility and flexibility have been developed to a high degree by the laboratory personnel in dealing with the many problems encountered in the nation's rapidly developing space systems. Expertise in the latest scientific developments is vital to the accomplishment of tasks related to these problems. The laboratories that contribute to this research are:

Aerophysics Laboratory: Launch vehicle and reentry fluid mechanics, heat transfer and flight dynamics; chemical and electric propulsion, propellant chemistry, environmental hazards, trace detection; spacecraft structural mechanics, contamination, thermal and structural control; high temperature thermomechanics, gas kinetics and radiation; cw and pulsed laser development including chemical kinetics, spectroscopy, optical resonators, beam control, atmospheric propagation, laser effects and countermeasures.

Chemistry and Physics Laboratory: Atmospheric chemical reactions, atmospheric optics, light scattering, state-specific chemical reactions and radiation transport in rocket plumes, applied laser spectroscopy, laser chemistry, laser optoelectronics, solar cell physics, battery electrochemistry, space vacuum and radiation effects on materials, lubrication and surface phenomena, thermionic emission, photosensitive materials and detectors, atomic frequency standards, and environmental chemistry.

Computer Science Laboratory: Program verification, program translation, performance-sensitive system design, distributed architectures for spaceborne computers, fault-tolerant computer systems, artificial intelligence and microelectronics applications.

Electronics Research Laboratory: Microelectronics, GaAs low noise and power devices, semiconductor lasers, electromagnetic and optical propagation phenomena, quantum electronics, laser communications, lidar, and electro-optics; communication sciences, applied electronics, semiconductor crystal and device physics, radiometric imaging; millimeter wave, microwave technology, and RF systems research.

Materials Sciences Laboratory: Development of new materials: metal matrix composites, polymers, and new forms of carbon; nondestructive evaluation, component failure analysis and reliability; fracture mechanics and stress corrosion; analysis and evaluation of materials at cryogenic and elevated temperatures as well as in space and enemy-induced environments.

Space Sciences Laboratory: Magnetospheric, auroral and cosmic ray physics, wave-particle interactions, magnetospheric plasma waves; atmospheric and ionospheric physics, density and composition of the upper atmosphere, remote sensing using atmospheric radiation; solar physics, infrared astronomy, infrared signature analysis; effects of solar activity, magnetic storms and nuclear explosions on the earth's atmosphere, ionosphere and magnetosphere; effects of electromagnetic and particulate radiations on space systems; space instrumentation.

END

FILMED

12-85

DTIC